Polypyrrole-Magnetite-Nanocomposite Based Toroidal Transformers: An Economical Industrial Solution with Minimum Core Losses

Jyoti Shah*, R K Kotnala

CSIR-National Physical Laboratory, Dr K S Krishnan Marg, Delhi, India

Volume 1, Issue 4, July 2024
Received:20 June, 2024; Accepted: 12 July, 2024
DOI: https://doi.org/10.63015/5N-2433.1.4

**Corresponding Author Email: shah.jyoti1@gmail.com*

Abstract: Electricity transmission and power conversion devices are always associated with huge power losses and transformer is the primary element in electricity transmission system and power conversion devices. Moreover, it is the major constituent of the power losses because of retaining substantial core losses which are further disintegrated into hysteresis and eddy current losses. Consequently, there is an immediate need for innovating new materials for transformer core to minimize the losses. Besides low hysteresis losses, high power to weight ratio is also a key factor for fabricating efficient and light weight transformer core. In this direction, soft magnetic nanocomposites provide attainable solution by exhibiting low hysteresis losses. In present work it is first time reporting a light weight and highly efficient polypyrrole-magnetite nanocomposite based toroidal transformer core. Polypyrrole-magnetite based nanocomposites are synthesized by facile and cost-effective solution phase route and fabricated as toroidal cores to study the power losses at high frequencies for transformer applications. Vibrating sample magnetometer (VSM) study shows the decrement in hysteresis losses from 8576 erg/cm^3 for bare Fe_3O_4 NPs to 6467 erg/cm^3 for NC-90(90:10; Fe_3O_4:PPy).Core losses measurement of composites at open circuit (no-load test) reveals reduction in loss values from 43.20 mW/cm^{3}for bare Fe_3O_4 NPs to 30.72 mW/cm^3 for NC-90 and from 30.35 mW/cm^3 to 18.24 mW/cm^{3}at 5 V and 3.5 V excitation voltages, respectively. Moreover, similar trends are also observed in broad range of frequencies ranging from 50 Hz to 50 kHz. Minimum core loss30.72 mW/cm^{3}at 50 kHz has been reported by NC-90 nanocomposite. Low Core losses are the primary need of hour for miniaturization of future economical transformer devices.

Keywords: Nanomagnetic particles, Hysteresis, Nanocomposite, Polypyrrole, Transformer core.

1. Introduction: Power saving has become a primary challenge for today's world due to fast deprivation of natural resources and emerging of deleterious environmental problems [1,2]. Transformers have major role for retaining the power owing to its vast applications in power and electronics industries such as power distribution and transmission systems, power converters in switching mode power supplies and as wide band and pulse transformers [3-5]. Core geometry, core material and the windings are the critical elements of the transformers that specify its efficiency, weight and cost [6]. Being the key parameter, core material plays the central role in power conversion in the transformer devices at global level**.** Electrical steel (Fe-Si alloy) and soft ferrites such as Mn-Zn, Ni-Zn and Mg-Zn ferrites are the traditional base materials of transformer cores due to their high saturation magnetic induction and low power losses for low and high frequency applications, respectively [7,8]. Electrical steel has low corrosion resistance with high processing cost [9-11] and micro-magnetic soft

ferrites have large volume of magnetic components and high hysteresis losses [12-15]. However, lack of significant and desirable power losses in case of these materials, limit their commercial viability and technological feasibility [1]. Consequently, there is continuous strong urge across the world for novel materials to achieve the adequate power losses. The strategic goal is to carry out the research for the development of light weight and easily processed soft magnetic nanocomposite materials for the fabrication of transformer core for advance technologies at minimal cost. Owing to their negligible coercivity, superparamagnetic nanoparticles of single domain are extremely advantageous for producing low hysteresis losses [16,17]. Soft ferrite nanoparticles dispersed in conducting polymer matrix offer high saturation magnetic induction, low power losses with tunable properties, ease of manufacturing and high corrosion resistance [18,19]. As per literature, bulk soft ferrites exhibit 288 mW/cm^3 power losses at high frequency of 50 kHz [20]. Recently, Zhou et al reported 450 mW/cm^3 power losses at 50 kHz frequency for composite core in which Fe-6.5wt% Si powder insulated with Mn-Zn ferrite nanoparticles [15]. Mori et al designed Ni-Zn-Fe ferrite coated with Fe-3.5 Si-4.5 Cr powder composite core showed 224 mW/cm^3 power losses at 50 kHz [21]. In present work toroidal cores have been fabricated using nanocomposite material, synthesized through a universally recognized simple solution method taking magnetite nanoparticles (Fe_3O_4 NPs) and polypyrrole as starting precursors. Transformer cores have been constructed into toroidal geometry to allow the maximum magnetic flux enclosure and to provide supports on its edges which subsequently minimizes core stress [6,22]**.** Being less toxic with good magnetic properties, facile synthesis and chemical stability of Fe_3O_4 NPs in conjunction with polypyrrole provided a unique platform of nanocomposites for the designing of highly efficient, light weight, cost effective core material with tunable functionalities and environmental benign synthesis protocols [23-28]. Synthesized nanocomposites exhibited good saturation magnetization with negligible coercivity. As a consequence, hysteresis losses were decreased due to reduction in surface anisotropy with the incorporation of polypyrrole as well as alternating current (AC) power losses were comparatively lower than pure Fe_3O_4 NPs at high frequencies [29]. Low power losses as well as high saturation magnetic induction properties were obtained in nanocomposite cores with light weight, ease of processing and low cost also. To the best of our knowledge, no work has been published on the synthesis of nanocomposite (Fe_3O_4 NPs and polypyrrole) involving DMSO as a solvent by solution synthesis method. In fact, it is first report on the fabrication of transformer toroidal cores of magnetite–polypyrrole nanocomposite.

2. Experimental Details

2.1. Materials

Ferrous chloride tetrahydrate ($FeCl_3.4H_2O$), ferric chloride hexahydrate ($FeCl_3.6H_2O$) and ammonia solution (25 %) of Merck were used in the experiments. Pyrrole and methanol were of analytical grade. Distilled water (DI water) was used for the experiments.

2.2. Preparation of Fe_3O_4 NPs by co-precipitation method

Fe_3O_4 NPs were prepared by co-precipitation method. Firstly, $FeCl_3.4H_2O$ and $FeCl_3.6H_2O$ with molar ratio (2:1) were dissolved in DI water. Ammonia solution (30 mL) was added drop wise under stirring into the reaction solution at maintained temperature of 70 °C and pH value of solution was adjusted at 12. Reaction solution was stirred for next 10 minutes. Prepared Fe_3O_4 NPs from reaction solution were washed with DI water and dried in vacuum oven at 60 °C for 8 hours.

2.3. Polymerization of Pyrrole by chemical oxidative polymerization method

Chemical oxidative polymerization method was adopted for polymerization of pyrrole. Pyrrole was distilled under reduced pressure and stored in dark at 5 °C. $FeCl_3.6H_2O$ oxidant (0.016 molar) was dissolved in DI water and oxidant solution was degassed before use. Distilled pyrrole (0.50 mL) was added into oxidant solution under vigorous stirring in argon atmosphere and was continued for next 8 hours. Prepared PPy was washed with methanol and dried in vacuum oven at 50 °C for 24 hours.

2.4. Formation of nanocomposites

Solution method was used for the formation of nanocomposites. As-prepared Fe_3O_4 NPs and PPy were dispersed in di-methyl sulfoxide (DMSO) solvent separately with the aid of probe sonicator for 45 minutes and 15 minutes, respectively. Fe_3O_4 NPs and PPy solutions were intermixed with the aid of probe sonicator for 20 minutes. Prepared nanocomposites solutions were mixed with water and then reaction mixture was separated from the DMSO and water solvent through magnetic decantation. Obtained reaction mixture was washed with DI water and dried in vacuum oven at 50 °C for 24 hours. As a result, five samples of nanocomposites were prepared with loading of Fe_3O_4 NPs in different concentration (8.6 g, 3.86 g, 2.24 g, 1.45 g and 0.967 g in DMSO solvent, respectively) in polypyrrole (0.967 g in DMSO solvent) matrix and samples were denoted NC-90 (90 % loading of Fe_3O_4 NPs in polypyrrole matrix), NC-80 (80% loading of Fe_3O_4 NPs in polypyrrole matrix), NC-70 (70% loading of Fe_3O_4 NPs in polypyrrole matrix), NC-60 (60% loading of Fe_3O_4 NPs in polypyrrole matrix) and NC-50 (50% loading of Fe_3O_4 NPs in polypyrrole matrix), respectively. Schematic representation of Fe_3O_4 NPs, PPy and nanocomposites synthesis are shown in Figure 1.

2.5. Characterization Techniques

X-ray diffraction analysis of the samples was examined on Rigaku make X-ray diffractometer with CuK_α (λ=1.54 Å) radiation source. CuK_α radiation was produced at room temperature with power setting of 40 kV and 30 mA. Infrared spectra of the prepared samples using the KBr pellet were recorded on Fourier Transform Infrared spectrometer (IR infinity-I Shimadzu). Particle size and morphology of the Fe_3O_4 NPs and nanocomposite samples were determined from high resolution transmission electron microscopy (HRTEM, Technai G20-stwin) at an accelerating voltage of 200 kV. Point and line resolution of HRTEM were 1.44 and 2.32 Å, respectively. A small drop of diluted Fe_3O_4 NPs and nanocomposite samples (NC-50 and NC-90) in ethanol were dripped on TEM grids for performing the TEM analysis. Magnetic measurements of nanocomposite samples were performed at room temperature using vibrating sample magnetometer (VSM, Lakeshore 7404**)** at an applied maximum external magnetic field of 5 kOe. The electrical conductivity of polypyrrole and nanocomposite samples was measured using four-point probe method. Conductivity measurement was performed on circular pellets of samples having diameter of 10 mm and thickness of 1 mm, prepared by hydraulic press. An open circuit test (no-load test) was executed using power meter on nanocomposite based toroidal cores. Nanocomposite samples were compacted into toroidal shaped specimens using hydraulic press having following dimensions (outer diameter = 14 mm, inner diameter = 7 mm and height = 4 mm) with the aid of polyvinyl alcohol (PVA).

3. Results and Discussion:

Crystallographic structures of prepared samples are presented in Figure 2. Crystalline peaks of Fe_3O_4 NPs at 2θ = 30.1°, 35.6°, 43.1°, 53.6°, 57.1° and 62.9° indexed to the (220), (311), (400), (422), (511) and (440) lattice planes, respectively which confirm the pure crystalline phase formation of Fe_3O_4 NPs (JCPDS-

790417). Using Scherrer's equation, the average particle size of Fe_3O_4 NPs is calculated 9.27 nm. Polypyrrole XRD pattern shows broad scattering peak at 25.8° diffraction angle determined its amorphous phase which is the characteristics of doped polypyrrole [30]. The peaks at 2θ = 30.1°, 35.6°, 43.1°, 53.6°, 57.1°, 62.9° and 25.8° reveal the presence of Fe_3O_4 NPs and polypyrrole in the nanocomposite samples [31]. Figure 3 depicts the FTIR spectra of polypyrrole, Fe_3O_4 NPs and nanocomposite samples. The absorption band at 576 cm^{-1} is attributed to Fe-O bond stretching in the Fe_3O_4 nanoparticles [32]. The characteristics peaks obtained at 3410 cm^{-1} and 1533 cm^{-1} are assigned to the N-H stretching and C-C stretching vibrations in the polypyrrole sample [33,34]. The absorption centered in the range (1250-1100) cm^{-1} is ascribed to the pyrrole ring vibration [26]. Peaks observed at 1294 cm^{-1} and 1031 cm^{-1} denote the C-H in plane and out of plane deformation mode. C=C stretching vibration in polypyrrole is occurred at 894 cm^{-1} [35]. The main absorption bands of polypyrrole and Fe_3O_4 NPs are appeared in the nanocomposite samples which confirm the existence of polypyrrole and Fe_3O_4 NPs. However, noticeable peak shifting is observed in the nanocomposite compared to bare magnetite nanoparticles and polypyrrole peaks. It may be attributed to non-covalent interactions such as columbic and Vanderwaal's interactions between the magnetite and polypyrrole [29,36,37]. Surface dangling bonds of magnetite interact with ring electron density of the polypyrrole. Moreover, such interactions induce a synergy effect in the final nanocomposite and resulted into the reduced resistivity and power losses. Such surface interactions promote the uniform dispersion of magnetic nanoparticles in polymer matrix observed in HRTEM images. HRTEM images of Fe_3O_4 NPs are shown in Figure 4 (a) and 4 (a′). Fe_3O_4 NPs are of spherical shape with average diameter of 9 nm similar to XRD crystallite size [31]. Figure 4 (b) and 4(b′) show the HRTEM micrographs of the NC-50 sample and Figure 4(c) and 4(c′) represent the HRTEM images of the NC-90 sample. A uniform dispersion of Fe_3O_4 NPs is observed in polypyrrole matrix [38]. Magnetization and flux density curves at room temperature are plotted as a function of magnetic field to study the magnetic properties of the prepared samples shown in Figure5(a) and 5 (b). Images of the flux density curves at low magnetic field are also incorporated in Figure 5 (b). Magnetic properties of the Fe_3O_4 NPs and nanocomposite samples are listed in Table 1. Magnetic properties such as saturation magnetization (M_s), coercivity (H_c), hysteresis area and magnetocrystalline anisotropy constant (K) of the nanocomposite samples were reduced because of the inclusion of non-magnetic polypyrrole polymer content. Magnetic properties of the magnetic nanoparticles are greatly affected by the surface chemistry [39]**.** Reduced magnetization in superparamagnetic nanoparticles is described based on the presence of disordered spins at the surface and by the spin canting [40]. Additionally, saturation magnetization is reduced in the nanocomposite samples with the incorporation of polypyrrole molecules due to predominant diamagnetic nature of polypyrrole[41].Furthermore, magnetic properties of magnetic NPs also depend on many anisotropy aspects. Dispersion of Fe_3O_4 NPs in polypyrrole matrix may influence surface anisotropy and interface anisotropy due to interfacial electrostatic and Vander-waals interactions [29]. The decrement in coercivity of the nanocomposite may be due to reduced surface anisotropy of Fe_3O_4 NPs by interfacial bonding of PPy ring electrons with its surface spins (dangling bonds). Using stoner-wohlfarth theory, the H_c of nanoparticles is calculated by the equation (1):

$$H_c = \frac{2K}{\mu_o M_s} \quad \text{..... (1)}$$

Herein, K is magneto crystalline anisotropy, μ_o is the permeability in free space and its value is

$4\pi\times10^{-7}$ H/m and M_s is the saturation magnetization. The value of K is determined by the product of H_c and M_s. It can be inferred that K value is monotonically decreasing function with loading of polypyrrole resulting into reduction of H_c and M_s. Thus, coercivity value varies with change in surface anisotropy. Consequently, hysteresis losses reduced. Figure 6 represents the conductivity values of the nanocomposite samples and polypyrrole. Conductivity decreases with increasing concentration of Fe_3O_4 NPs in the nanocomposite samples. Conduction mechanism in the conducting polymer arises due to transport mechanism of anions, bipolarons and hopping of electrons in its conjugated system. Charge carrier scattering and blockage of conduction path, both are enhanced with the inclusion of the Fe_3O_4 NPs in the polypyrrole matrix as well as free surface charge is decreased due to physical interaction between polypyrrole and Fe_3O_4 magnetic NPs. Consequently, conductivity is reduced [42-45]. Figures 7 and 8 demonstrate the power losses density curves of the samples as a function of frequency from 50 Hz to 50 kHz at two sinusoidal exciting voltages 5 V and 3.5 V, respectively. Power losses are segregated into three components: hysteresis losses (P_h), eddy current losses (P_e) and residual losses (P_r). Residual losses predominate only at very high frequencies and at low magnetic flux density levels [46]. It is approximated to zero in the power applications of the soft magnetic materials [47,48]. Hysteresis losses are appeared due to high coercivity of the magnetic materials and surface anisotropy determines the coercivity factor as above discussed [22,39,49]. With the incorporation of polymer content in the Fe_3O_4 magnetic NPs, coercivity was reduced and hysteresis losses were decreased. It can be validated by the calculated values of the coercivity and hysteresis area as displayed in Table 1. On the other side, eddy current losses are increased due to decrement in resistivity with the addition of polymer content [22]. Resistivity of the nanocomposite samples is decreased with the inclusion of higher concentration of polypyrrole and it is shown in Figure 6. Eddy current losses are comparable to the hysteresis losses at normal line frequency (50 Hz/60 Hz) [22]. P_e is directly proportional to the square of frequency while P_h is directly proportional to the frequency. Accordingly, eddy current losses are abruptly enhanced than hysteresis losses with the increased excitation frequency [50]. Consequently, power losses are almost constant till 1 kHz frequency and increased beyond 1 kHz frequency as shown in Figures 7 and 8. Power loss density values at 50 Hz frequency were decreased from 37.80 mW/cm^3 for Fe_3O_4 magnetic NPs to 24.58 mW/cm^3 for NC-90 sample at 5 V and also reduced from21.41 $mW/cm^3$to 14.71 mW/cm^3 at 3.5 V. Power loss density values at 50 kHz decreased from 43.20 mW/cm^3 (Fe_3O_4 magnetic NPs) to 30.72 mW/cm^3 (NC-90 sample) at 5 V and it is reduced from 30.35 mW/cm^3 to 18.34 mW/cm^3 at 3.5 V excitation voltages. Power loss density values were further increased from 24.58 mW/cm^3 and 14.71 mW/cm^3 (NC-90) to 34.45 mW/cm^3 and 18.99 mW/cm^3 (NC-50 sample) at 5 V and 3.5V excitation voltages, respectively at 50 Hz frequency. Power losses density values were also further increased from 30.72 mW/cm^3 and 18.34 mW/cm^3 (NC-90 sample) to 40.40 mW/cm^3 and 29.93 mW/cm^3 (NC-50 sample) at 5 V and 3.5V excitation voltages, respectively at 50 kHz frequency, but still less than the Fe_3O_4 magnetic NPs. It might be increased due to enhancement of eddy current losses with the decrement in resistivity. Resistivity is reduced with the loading of polypyrrole in nanocomposite due to induced synergy effect via non covalent interaction between ring electron density of the polypyrrole and surface dangling bonds of magnetite. Additionally, conduction takes place with the inclusion of conducting polypyrrole phase in nanocomposite. Consequently, eddy current gets conduction path easily and eddy current losses are enhanced rapidly.

4. Conclusions

This work reports an eloquent approach for reducing core losses at high frequencies by nanocomposite of Fe_3O_4 NPs and PPy. At high frequency of 50 kHz, power loss density values decreased from 43.20 mW/cm^3 (Fe_3O_4 magnetic NPs) to 30.72 mW/cm^3 (NC-90 sample) at 5 Vand it reduced from 30.35 mW/cm^3 to 18.34 mW/cm^{3}at 3.5 V excitation voltages. Reduction in core losses in nanocomposite is the result of decrease in coercivity of nanocomposite. Core losses monotonically increased with polypyrrole concentration. Therefore, the core losses were increased in NC-50 sample comparatively to NC-90 sample. Enhancement in eddy current losses may be the reason for increased core losses because the conductivity is increased with the addition of polypyrrole phase in nanocomposite. Trivial hysteresis losses obtained in nanocomposite due to reduced surface anisotropy by interfacial surface interaction of PPy and Fe_3O_4 NPs. Nanocomposite sample (NC-90) with less inclusion of PPy matrix exhibited minimum core loss at high frequency, which is most suited for switching mode power supplies.

References

[1] D. van Niekerk, B. Schoombie and P. Bokoro, Design of an Experimental Approach for Characterization and Performance Analysis of High-Frequency Transformer Core Materials, *Energies* **16(9)**, 2023, 3950.

[2] K. Zhu, H. Chen, S. Li, C. Sun, F. Liu, An RF On-Chip Transformer With Fe_3O_4/GO Nanocomposite Film, *IEEE Transactions on Magnetics*, **57**, 2, 2021.

[3] A. Najafi, and I. Iskender, Comparison of core loss and magnetic flux distribution in amorphous and silicon steel core transformers. *Electr. Eng.***100**, 2018, 1125–1131.

[4] R. Williams, D. A. Grant, and J. Gowar, Multielement transformers for switched-mode power supplies: toroidal designs. *IEE Proc. B Electr. Power Appl.***140**, 1993, 152.

[5] A. C. Razzitte, S. E. Jacobo, and W. G. Fano, Magnetic properties of MnZn ferrites prepared by soft chemical routes. *J. Appl. Phys.***87**, 2000, 6232–6234.

[6] L. M. Bollig, P. J. Hilpisch, G. S. Mowry, and B. B. Nelson-Cheeseman, 3D printed magnetic polymer composite transformers. *J. Magn. Magn. Mater.***442**, 2017, 97–101.

[7] Z. H.Khan, M. Rahman, S. S. Sikder, M. A. Hakim, and D. K. Saha, Complex permeability of Fe-deficient Ni–Cu–Zn ferrites. *J. Alloys Compd.* **548**, 2013, 208–215.

[8] Y. Lu, G. Zu, L. Liu, Y. Wang, L. Gao, L.Yuan, X. Ran, X. Zhang, Investigation of microstructure and properties of strip-cast 4.5 wt% Si non-oriented electrical steel by different rolling processes. *J. Magn. Magn. Mater.* **497**, 2020, 165975.

[9] J. E. Contreras, E. A. Rodriguez, and J. Taha-Tijerina, Nanotechnology applications for electrical transformers—A review. *Electr. Power Syst. Res.* **143**, 2017, 573–584.

[10] G. Ouyang, X. Chen, Y. Liang, C. Macziewski, and J. Cui, Review of Fe-6.5 wt%Si high silicon steel—A promising soft magnetic material for sub-kHz application. *J. Magn. Magn. Mater.***481**, 2019, 234–250.

[11] H. Wayne Beaty, Donald Fink. *Standard Handbook for Electrical Engineers (2012)*.

[12] K. Praveena, K. Sadhana, S. Bharadwaj, and S. R. Murthy, Development of nanocrystalline Mn–Zn ferrites for forward type DC–DC converter for switching mode power supplies. *Mater. Res. Innov.***14**, 2010 56–61.

[13] J. Gass, Functional Magnetic Nanoparticles. (University of South Florida, 2012).

[14] G. Khan, Design and synthesis of soft magnetic materials for high frequency power applications. (Dartmouth College, 2014).

[15] M. M. Zhou, *et al.* Magnetic properties and loss mechanism of Fe-6.5wt%Si powder core insulated with magnetic Mn-Zn ferrite nanoparticles. *J. Magn. Magn. Mater.***482**, 2019, 148–154.

[16] Z. Mosleh, P. Kameli, M. Ranjbar, and H. Salamati, Effect of annealing temperature on structural and magnetic properties of $BaFe_{12}O_{19}$ hexaferrite nanoparticles. *Ceram. Int.***40**, 2014, 7279–7284.

[17] M. Houshiar, F. Zebhi, Z. J. Razi, A. Alidoust, and Z. Askari, Synthesis of cobalt ferrite ($CoFe_2O_4$) nanoparticles using combustion, coprecipitation, and precipitation methods: A comparison study of size, structural, and magnetic properties. *J. Magn. Magn. Mater.***371**, 2014, 43–48.

[18] Yun, H. *et al.* Size and composition dependent radio frequency magnetic permeability of iron

oxide nanocrystals. *ACS Nano* **2014**, 12323–12337.

[19] S. C. Mills, E. A. Patterson, J. S. Andrew, 0-3 magnetic nanocomposites via EPD: Current status for power component fabrication and future directions, *Am Ceram Soc.* **107(3)**, 2024, 1859–1870.

[20] J. P. F. Araújo, High power density DC-DC converter. 2015.

[21] S. Mori, T. Mitsuoka, M. Sonehara, T. Sato, & N. Matsushita, High permeability and low loss of Ni-Zn-Fe ferrite/metal composite cores in high frequency region. *AIP Adv.***7**, 2017, 056657.

[22] H. W. Ng, R. Hasegawa, A. C. Lee, & L. A. Lowdermilk, Amorphous alloy core distribution transformers. *Proc. IEEE* **79**, 1991, 1608–1623.

[23] V. F. Cardoso, A. Francesko, C. Ribeiro, M. Bañobre-López, P. Martins, S. Lanceros-Mendez, Advances in Magnetic Nanoparticles for Biomedical Applications, *Advanced Healthcare Materials*, **7(5),** 2018, 17000845.

[24] N. A. Frey, S. Peng, K. Cheng, and S. Sun, Magnetic nanoparticles: synthesis, functionalization, and applications in bioimaging and magnetic energy storage. *Chem. Soc. Rev.***38**, 2009, 2532.

[25] S.-J. Yen, E.-C.Chen, R.-K. Chiang, & T.-M. Wu, Preparation and characterization of polypyrrole/magnetite nanocomposites synthesized byin situ chemical oxidative polymerization. *J. Polym. Sci. Part B Polym. Phys.***46**, 2008, 1291–1300.

[26] M. Wysocka-Żołopa, A. Brzózka, E. Zambrzycka-Szelewa, U. Klekotka,·B. Kalska-Szostko, K. Winkler, Structure and electrochemical properties of magnetite and polypyrrole nanocomposites formed by pyrrole oxidation with magnetite nanoparticles, *Journal of Solid State Electrochemistry*, **27**, 2023, 1919–1934.

[27] Y.He, Dai, X. Zhang, Y. Sun, W. Shi, D. Ge The Bioactive Polypyrrole/Polydopamine Nanowire Coating with Enhanced Osteogenic Differentiation Ability with Electrical Stimulation, *Coatings* **10(12)**, 2020, 1189.

[28] Md. K. Hossain, Md. M. Hasan, Md. S. Islam, O. T. Mefford, H. Ahmad, and Md. M. Rahman, Polypyrrole Coating via Lemieux-von Rudloff Oxidation on Magnetite Nanoparticles for Highly Efficient Removal of Chromium(VI) from Wastewater, *ACS Omega* **9,** 2024, 17, 19077–19088.

[29] Y.-L. Luo, Li-H. Fan, F. Xu, Y.-S. Chen, C.-Hu Zhang, Q.-Bo Wei, Synthesis and characterization of Fe_3O_4/PPy/P(MAA-co-AAm) trilayered composite microspheres with electric, magnetic and pH response characteristics. *Mater. Chem. Phys.***120**, 2010, 590–597.

[30] K. Cheah, M. Forsyth, V.-T. Truong, Ordering and stability in conducting polypyrrole. *Synth. Met* .**94**, 1998, 215–219.

[31] H. Zhang, X. Zhong, J.-J. Xu, and H.-Y. Chen, Fe_3O_4 /Polypyrrole/Au Nanocomposites with Core/Shell/Shell Structure: Synthesis, Characterization, and Their Electrochemical Properties. *Langmuir* **24**, 2008, 13748–13752.

[32] M. T. Ramesan, Preparation and Properties of Fe_3O_4 /Polypyrrole/Poly(Pyrrole-Co-Acrylamide) Nanocomposites. *Int. J. Polym. Mater.***62**,2013, 277–283.

[33] V. V. Karambelkar, J. D. Ekhe, and S. N. Paul, High yield polypyrrole: A novel approach to synthesis and characterization. *J. Mater. Sci.***46**, 2011, 5324–5331.

[34] N. Arsalani, and K. E. Geckeler, Novel electrically conducting polymer hybrids with polypyrrole. *React. Funct. Polym.***33**, 1977, 167–172.

[35] L. G. Wade, *Organic chemistry*. Pearson Education India, 2008.

[36] J. Guo, H. Gu, H. Wei, Q. Zhang, N. Haldolaarachchige, Y. Li, D. P. Young, S. Wei and Z. Guo Magnetite–Polypyrrole Metacomposites: Dielectric Properties and Magnetoresistance Behavior. *J. Phys. Chem. C***117**, 2013, 10191–10202.

[37] F. F. Fang, Y. D. Liu, & H. J. Choi, Electrorheological and magnetorheological response of polypyrrole/magnetite nanocomposite particles. *Colloid Polym. Sci.***291**, 2013, 1781–1786.

[38] S. Varshney, A. Ohlan, V. K. Jain, V. P. Dutta, and S. K. Dhawan, Synthesis of ferrofluid based nanoarchitectured polypyrrole composites and its application for electromagnetic shielding. *Mater. Chem. Phys.***143**, 2014, 806–813.

[39] C. R. Vestal, and Z. J. Zhang, Effects of Surface Coordination Chemistry on the Magnetic Properties of $MnFe_2O_4$ Spinel Ferrite Nanoparticles. *J. Am. Chem. Soc.***125**, 2003, 9828–9833.

[40] E. Karaoğlu, Baykal, H. Deligöz, M. S¸enel, H. Sözeri, M.S. Toprak, Synthesis and characteristics of poly (3-pyrrol-1-ylpropanoic acid) (PPyAA)–Fe_3O_4 nanocomposite. *J. Alloys Compd.* **509**, 2011, 8460–8468.

[41] P. Xu, X. Han, C. Wang, H. Zhao, J. Wang, X. Wang and B. Zhang, Synthesis of Electromagnetic Functionalized Barium Ferrite Nanoparticles Embedded in Polypyrrole. *J. Phys. Chem. B* **112**, 2008, 2775–2781.

[42] K. R. Reddy, K. P. Lee, and A. I. Gopalan, Self-assembly approach for the synthesis of electro-magnetic functionalized Fe3O4/polyaniline nanocomposites: Effect of dopant on the properties. *Colloids Surf. Physicochem. Eng. Asp.***320**, 2008, 49–56.

[43] J. Deng, X. Ding. W. Zhang, Y. Peng, J. Wang, X. Long, P. Li, A. S. C. Chan, Magnetic and conducting Fe_3O_4 –cross-linked polyaniline nanoparticles with core–shell structure. *Polymer* **43**, 2002, 2179–2184.

[44] K. Singh, A. Ohlan, R. K. Kotnala, A. K. Bakhshi, and S. K. Dhawan, Dielectric and magnetic properties of conducting ferromagnetic composite of polyaniline with γ-Fe_2O_3 nanoparticles. *Mater. Chem. Phys.***112**, 2008, 651–658.

[45] R. Turcu, O. Pana, A Nan, I Craciunescu, O Chauvet and C Payen Polypyrrole coated magnetite nanoparticles from water based nanofluids. *J. Phys. Appl. Phys.***41**, 2008, 245002.

[46] L. Chang, L. Xie, M. Liu, Q. Li, Y. Dong, C. Chang, X.-M. Wang and A. Inoue, Novel Fe-based nanocrystalline powder cores with excellent magnetic properties produced using gas-atomized powder. *J. Magn. Magn. Mater.***452**, 2018, 442–446.

[47] J. R. Brauer, Z. J. Cendes, B. C. Beihoff, and K. P. Phillips, Laminated steel eddy current loss versus frequency computed using finite elements. *IEEE Trans. Ind. Appl.***36**, 2000, 1132–1137.

[48] X. Li, J. Zhou, L. Shen, B. Sun, H. Bai, W. Wang, Exceptionally High Saturation Magnetic Flux Density and Ultralow Coercivity via an Amorphous–Nanocrystalline Transitional Microstructure in an FeCo-Based Alloy, *Advanced Materials* **35**, 2023, 2205863.

[49] T., Suetsuna, S. Suenaga, & Harada, K. Bulk nanogranular composite of magnetic metal and insulating oxide matrix. *Scr. Mater.***113**, 201), 89–92.

[50] S. Mori, T. Mitsuoka, K. Sugimura, R. Hirayama, M. Sonehara, T. Sato, N. Matsushita, Core-shell structured Mn-Zn-Fe ferrite/Fe-Si-Cr particles for magnetic composite cores with low loss. *Adv. Powder Technol.* **29**, 2018, 1481–1486.

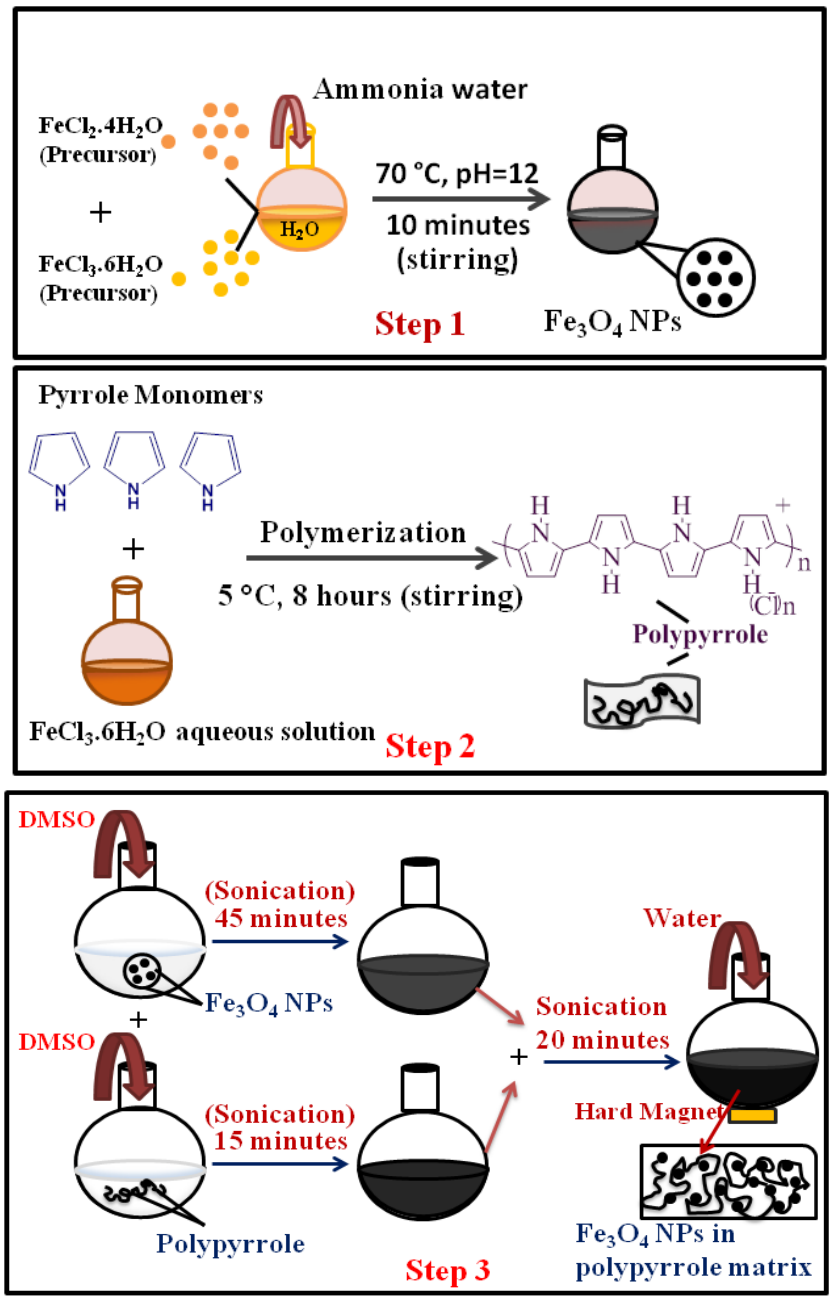
Ammonia water
FeCl2.4H2O
(Precursor)
+
FeCl3.6H2O
(Precursor)
H2O
70 °C, pH=12
10 minutes
(stirring)
Step 1
Fe3O4 NPs
Pyrrole Monomers
+
Polymerization
5 °C, 8 hours (stirring)
Polypyrrole
FeCl3.6H2O aqueous solution
Step 2
DMSO
(Sonication)
45 minutes
Fe3O4 NPs
+
DMSO
(Sonication)
15 minutes
Polypyrrole
+
Sonication
20 minutes
Water
Hard Magnet
Fe3O4 NPs in
polypyrrole matrix
Step 3

Figure 1

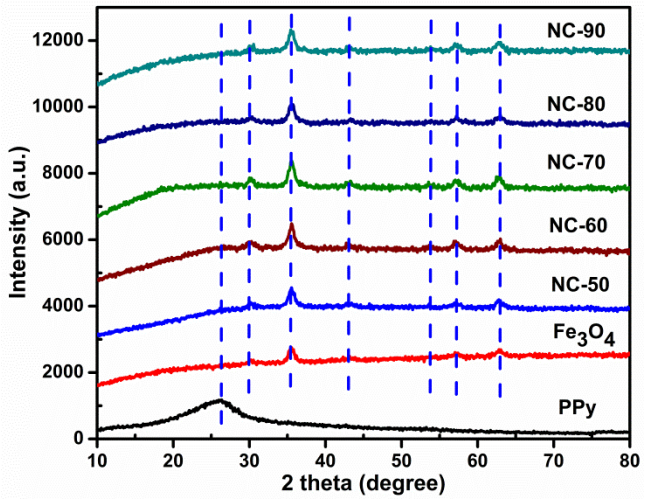

Figure 2

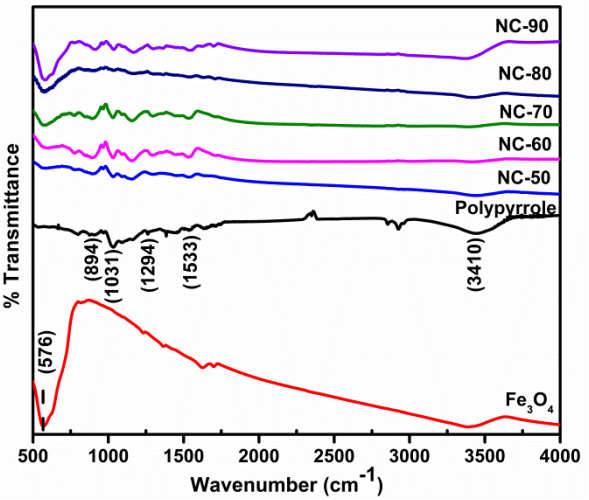

Figure 3

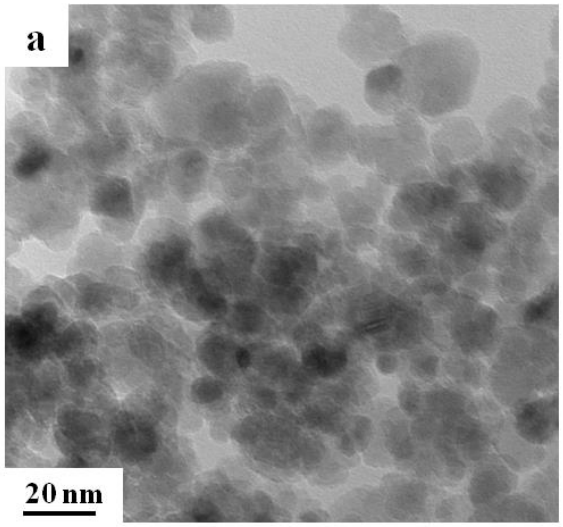

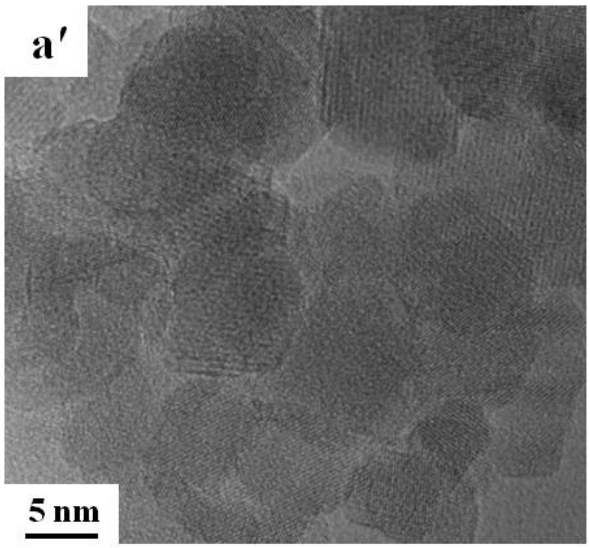

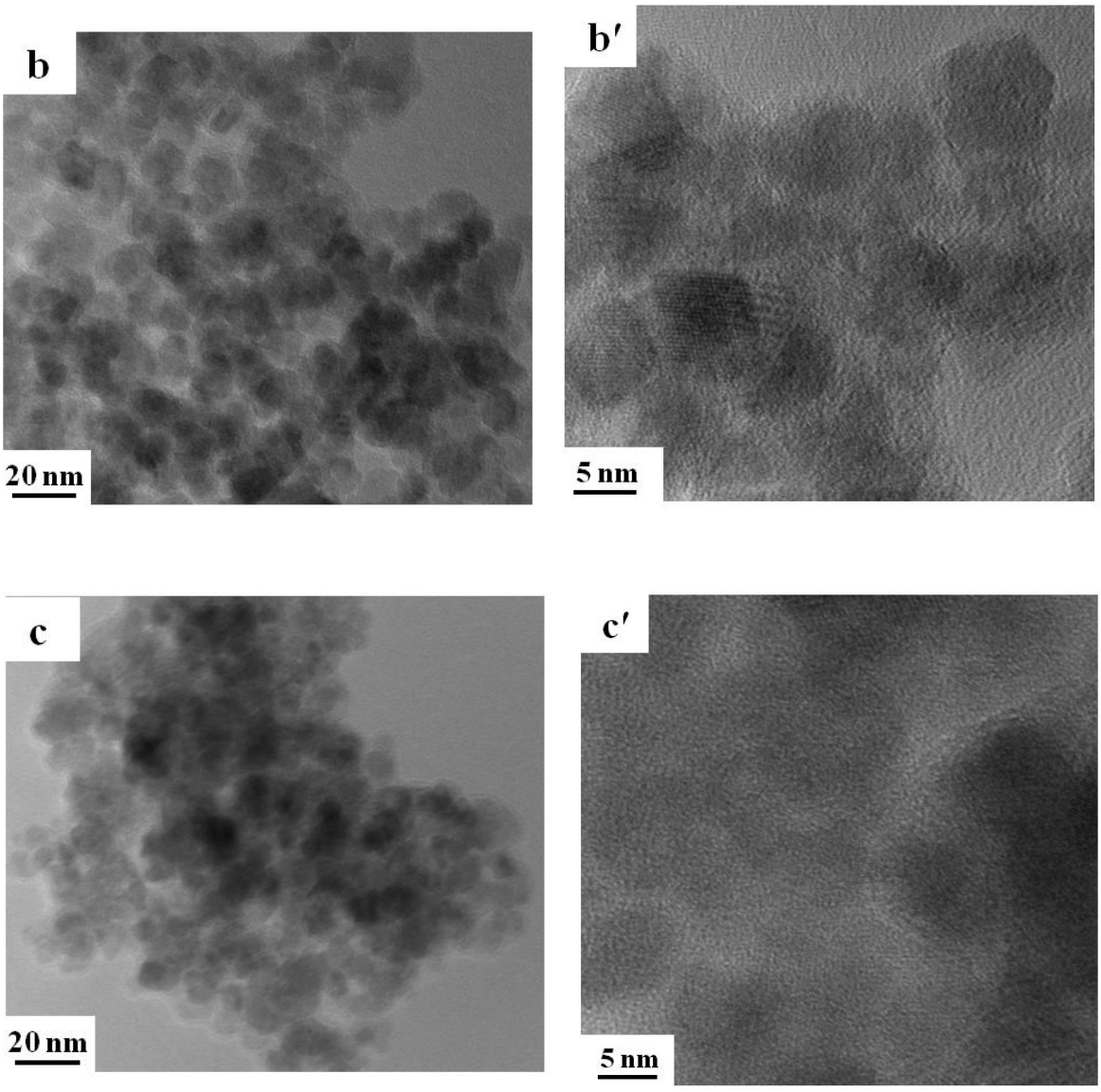

Figure 4

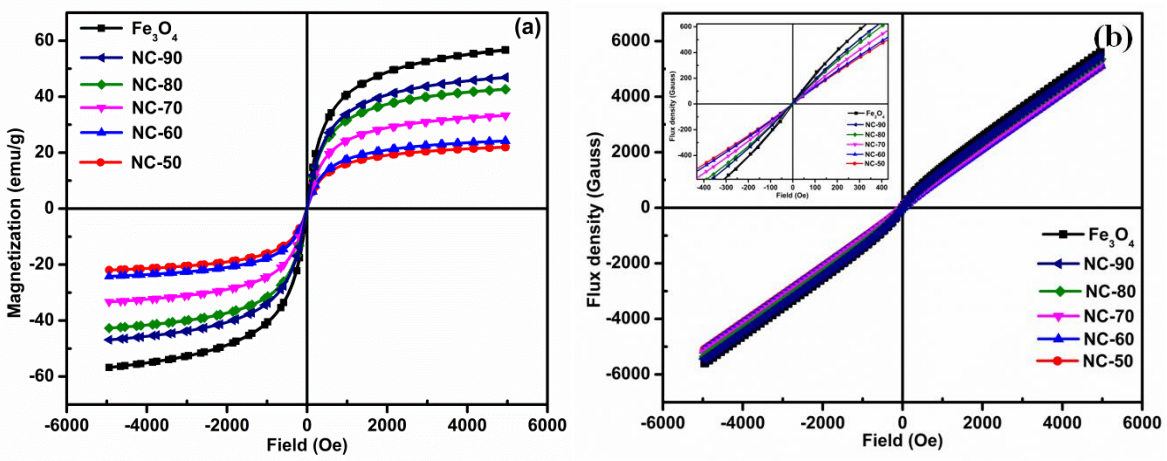

Figure 5

Table 1

	Saturation magnetization (M_s) (emu/g)	Saturation flux density (B_s)(Gauss)	Coercivity (H_c) (Oe)	Hysteresis losses (erg/cm^3)	K×μ_o
Fe_3O_4NPs	56.6	5,600	6.87	8576	388
NC-90	46.7	5,500	5	6467	233.5
NC-80	42.7	5,400	4	5367	170.8
NC-70	33.2	5,300	3.74	4558	124.16
NC-60	24.1	5,200	2.93	3751	70.613
NC-50	21.9	5,100	2.28	2455	49.932

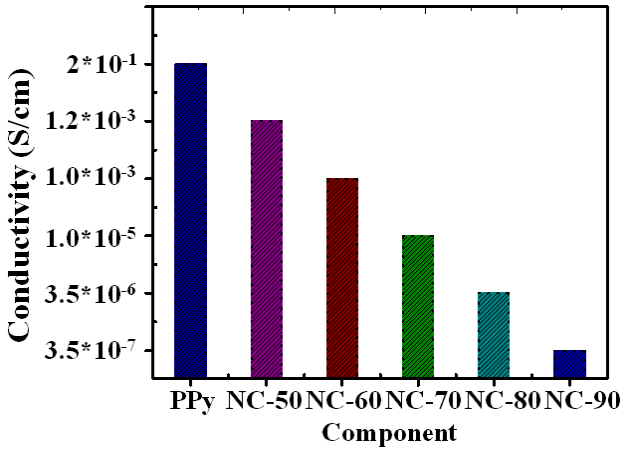

Figure 6

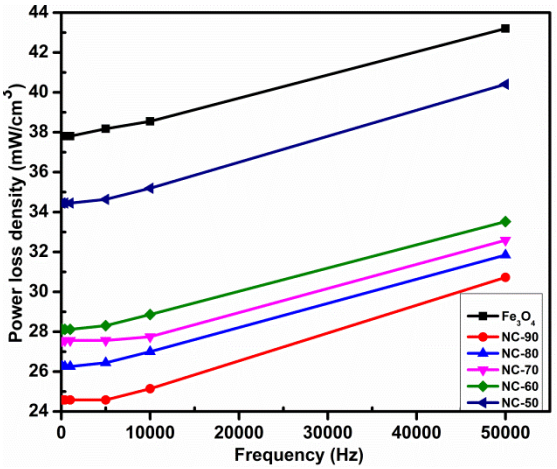

Figure 7

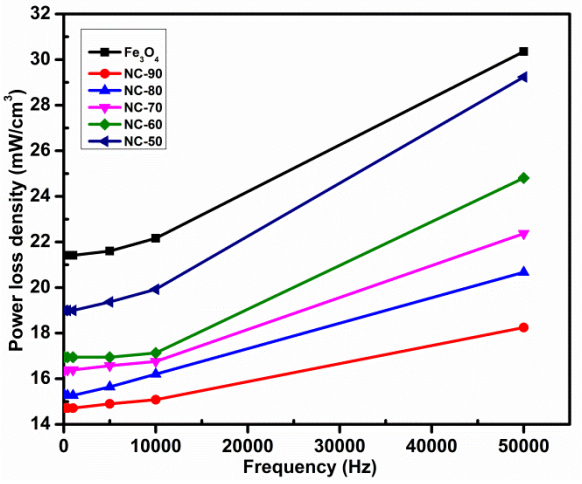

Figure 8